Metal–Organic Frameworks

DOI: 10.1002/anie.201100372

Dramatically Different Conductivity Properties of Metal–Organic Framework Polymorphs of Tl(TCNQ): An Unexpected Room-Temperature Crystal-to-Crystal Phase Transition**

*Carolina Avendano, Zhongyue Zhang, Akira Ota, Hanhua Zhao, and Kim R. Dunbar**

The synthesis and fabrication of nanoscale materials for new types of electronic and magnetic devices is a central theme in materials science research in this second decade of the 21st century. Given that conventional storage materials are estimated to approach their miniaturization limit by 2016,[1] heightened efforts are being directed at the design and synthesis of new types of bistable nanoscale materials, including those capable of undergoing a change from low to high resistance under the application of an electric field. Such nonvolatile memory devices are capable of operating at increased speeds and require less energy than conventional memory devices. Among the materials being investigated for resistance-based memory are materials that contain organic components and whose properties are influenced by magnetic or electric fields.[2]

Materials that respond to the application of an electric field or changes in light, pressure, or temperature are being sought for incorporation into electronic devices with ultrafast operating speeds.[3,4] Examples of molecule-based materials that exhibit fascinating properties are the spin-crossover complex $[Fe(picolylamine)_3Cl_2(C_2H_5OH)]$,[5,6] the neutral–ionic transition system TTF–chloranil (TTF = tetrathiafulvalene),[7–9] the metallo-organic conductor Cu(DM-DCNQI)$_2$,[10–16] (DM-DCNQI = dimethyl-*N*,*N*′-dicyanoquinonediimine) and the salt (EDO-TTF)$_2$PF$_6$,[17,18] (EDO-TTF = ethylenedioxytetrathiafulvalene). These materials provide compelling evidence for the contention that molecular solids may eventually be useful in device applications.

In terms of electric-field-induced behavior, the most extensively studied examples are the organocyanide-based materials Cu(TCNQ) (TCNQ = 7,7,8,8-tetracyanoquinodimethane), which exhibits reversible switching from a high-resistance state to a conducting state promoted by the application of an electric field or upon irradiation,[19–21] and the current-driven conductor K(TCNQ) salt.[22] The latter material is a key member of the binary series of alkali-metal salts of TCNQ that behave as so-called "Mott insulators" at high temperatures, in which the fully reduced radical anions are arranged in columns with evenly spaced TCNQ units. At lower temperatures, these "soft" materials undergo a phase transition in which the TCNQ units are brought into close proximity as a result of π dimerization. The electrons are then trapped in the dimers, the conductivity drops, and the materials pass into the spin-Peierls insulating state.

An approach that we have adopted for discovering conducting TCNQ phases is to capitalize on the rich chemistry of alkali metals while circumventing some issues that hinder their conductivity. In this vein, thallium is an interesting element, since it can behave as a pseudo-alkali metal. In contrast to other Group 13 elements, Tl prefers the 1+ oxidation state (although Tl^{3+} is known), and many similarities between the chemistry of alkali-metal ions and Tl^+ have been noted.[23] The electronegativity of Tl (2.04) is much higher than that of any alkali metal, which should lead to less ionic compounds with smaller band gaps and thus higher carrier mobility. Moreover, unlike alkali metals, Tl^+ possesses a stereoactive lone pair, which is expected to lead to a greater diversity of structures.[24] Indeed, the viability of this idea was demonstrated by Hünig et al., who reported Tl(DM-DCNQI)$_2$, which adopts a 3D metal–organic framework structure and behaves as a one-dimensional metal-like semiconductor ($\sigma_{300\,K} = 50\ S\,cm^{-1}$).[25]

With the exception of the aforementioned material, there are no other reported main-group binary phases based on weak interactions with organocyanide molecules. In fact, main-group supramolecular chemistry is largely underdeveloped as compared to that of transition-metal ions.[26–28] Herein we describe the first chemistry of the Tl^I cation with TCNQ radical anions, the result of which is the discovery of two polymorphs with very different conducting properties.

Slow diffusion of a methanol solution of Li(TCNQ) and an aqueous solution of $TlPF_6$ leads to the isolation of single crystals of the product Tl(TCNQ), phase I (**1**). A typical bulk stoichiometric reaction leads to crystals of a second product Tl(TCNQ), phase II (**2**). An X-ray structural determination revealed that **1** crystallizes in the $P2_1/c$ space group as a 3D network structure consisting of metal ions arranged in linear strings, each surrounded by four stacks of TCNQ acceptor molecules (Figure 1a) and with adjacent TCNQ stacks

[*] Dr. C. Avendano, Z. Zhang, Dr. A. Ota, Dr. H. Zhao, Prof. K. R. Dunbar
Department of Chemistry, Texas A&M University
P.O. Box 30012, College Station, TX 77842 (USA)
Fax: (+1) 979-845-7177
E-mail: dunbar@mail.chem.tamu.edu

[**] We acknowledge Nattamai Bhuvanesh for useful discussions. Use of the Advanced Photon Source at Argonne National Laboratory was supported by the U.S. Department of Energy, Office of Science, Office of Basic Energy Sciences, under Contract No. DE-AC02-06CH11357. This research was supported by the National Science Foundation (CHE-0957840) and, in part, by the Welch Foundation (A-1449). The data collected at Argonne National Laboratories were supported by the proposal GUP 13132. TCNQ = 7,7,8,8-tetracyanoquinodimethane.

Supporting information for this article is available on the WWW under http://dx.doi.org/10.1002/anie.201100372.

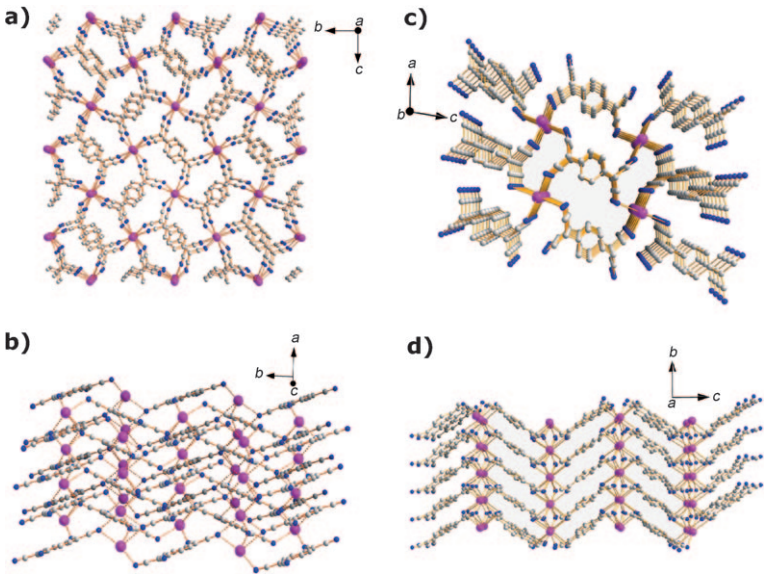

Figure 1. A perspective view of the crystal structure along the short axis of TlTCNQ a) Phase I (**1**) and c) Phase II (**2**) and side views of the crystal structures of b) Phase I (**1**) and d) Phase II (**2**) emphasizing the chains of Tl ions that are aligned in parallel directions.

rotated by 90° with respect to each other, as in the case of Cu(TCNQ) phase I. In contrast to the latter, the TCNQ units in **1** propagate along the *a* axis with alternating distances of 3.16(1) and 3.35(1) Å between the π systems along the stacks (Figure S1 in the Supporting Information). Each Tl^I center is coordinated to eight TCNQ molecules and has a stereoactive lone pair that forces the Tl^I centers to be in a distorted cubic geometry (Tl–N 2.70–3.27 Å). The distance between adjacent Tl metal ions along the short axis alternates between 3.46(1) and 3.70(1) Å.

Crystals of phase II (**2**) could only be obtained as very small crystallites, thus X-ray structural data were collected at the ChemMatCars APS synchrotron facility at Argonne National Laboratories. Polymorph **2** crystallizes in the *P*2/*c* space group in a 3D network whose structure consists of Tl ions surrounded by four stacks of TCNQ acceptor molecules, as found in **1** (Figure 1b), but with adjacent TCNQ stacks arranged in a parallel orientation with respect to each other (Figure 1d). Another important difference between the polymorphs is that the distances between the adjacent TCNQ radical and adjacent Tl metal ions in polymorph **2** are equivalent (3.22(2) and 3.79(2) Å, respectively; Figure S2 in the Supporting Information), a situation that leads to even spacings of π–π interactions throughout the stacks which propagate along the *b* axis. As in the case of **1**, the Tl centers in **2** adopt a distorted cubic coordination environment, as was indicated by the inequivalent Tl–N bond lengths (Figure S3 in the Supporting Information). The larger disparities in the Tl–N bond lengths for **1** illustrate a higher degree of distortion than found in **2**. The elongated Tl–N bonds (red in Figure S3 in the Supporting Information) observed for both polymorphs reflect the presence of Tl s-orbital lone-pair electrons. Furthermore, in both structures the distance between metal ions is slightly less than the sum of the van der Waals radii of two Tl^I ions (3.92 Å). Interactions between Tl atoms are quite rare and have only been documented in two other Tl supramolecular assemblies, namely $Tl(DM\text{-}DCNQI)_2$ (3.81 Å) and Tl_2(phthalocyanine) (3.69 Å). In both cases the Tl···Tl contacts are longer than those observed in the two new Tl(TCNQ) phases.[25,29]

It is well known that Tl^I compounds exhibit structural and chemical properties similar to corresponding K^+ and Ag^+ salts (Table 1). A comparison of the ionic radii reveals that the crystal structures of the different radical ion salts are not determined solely by the sizes of the metal ions. Whereas in the series M(TCNQ) (M^I = Na, K, Rb) the space group changes as the ionic radius increases ($C\bar{1}$, $P2_1/n$, and $P\bar{1}$ respectively), similar space groups are found for both the Cu(TCNQ) phase I and Ag(TCNQ) metal–organic framework solids (Table 1). It is obvious that the structural differences are not driven primarily by preferred distances between the acceptor molecules, because they would remain unchanged given that they are governed by the size of the TCNQ moiety. Instead, structural variations can be attributed to the different metal–nitrile group distances, *d*(M–N), which are shortest for the Cu, Ag, and Tl TCNQ compounds based on the sum of the van der Waals radii. In contrast, for the alkali-metal TCNQ materials, *d*(M–N) is equal to the sum of the van der Waals radii. As stated, the Tl(TCNQ) polymorphs exhibit metal–nitrogen distances considerably less than the sum of the van der Waals radii, an indication of increased bonding interactions of the nitrile groups compared to the purely electrostatic interactions found for alkali-metal TCNQ compounds. This situation notwithstanding, the new compounds **1** and **2** bear structural similarities to the alkali-metal TCNQ materials. The Tl^+ ion environment in **1** and **2** exhibits the characteristic coordination number eight of the K^+ ion, as opposed to the typical fourfold coordination exhibited by the Cu(TCNQ) and Ag(TCNQ) MOFs. The 90° arrangement of adjacent TCNQ stacks in **1** occurs in the structures of the Na^+, K^+, and Rb^+

Table 1: Metrical data and room-temperature conductivities for M(TCNQ) compounds.[a]

M, phase	r_i	$r_i + r_N$	*d*(M–N)	*d*(A–A)	σ_{300K}	Ref.
Cu, I	0.60	2.10	1.95	3.24	2.5×10^{-1}	[21]
Ag	1.00	2.50	2.33	3.50	3.6×10^{-4}	[30]
Tl, I	1.59	3.09	2.75	3.16/3.35	2.4×10^{-4}	
Tl, II	1.59	3.09	2.92	3.22	5.4×10^{-1}	
Na	1.02	2.52	2.50	3.22/3.50	1.0×10^{-5}	[31]
K	1.59	3.09	3.01	3.24/3.57	1.0×10^{-5}	[22]
Rb, II	1.65	3.15	3.08	3.25	1.0×10^{-5}	[32]

[a] r_i = ionic radius (Å), $r_i + r_N$ = sum of van der Waals radii (Å) of the cation and N atoms, *d*(M–N) = shortest distance between metal ion and nitrile N atom (Å), *d*(A–A) = average distance between acceptor molecules (Å), σ_{300K} = room-temperature conductivity ($S^{-1}cm^{-1}$). Nitrogen radius r_N = 1.50 Å.

TCNQ analogues, whereas the parallel arrangement of the TCNQ stacks found in **2** is observed in the Cs(TCNQ) network. Interestingly, the arrangement of the TCNQ radicals in polymorph **1** is the same as in the Cu(TCNQ) and Ag(TCNQ) structures, but, in the case of polymorph **1**, there is an uneven spacing of the π-stacked TCNQ radicals.

During the course of our studies of compound **1**, a surprising discovery was made. When a crystalline sample of **1** is exposed to moist laboratory air, a solid-to-solid phase change takes place for crystalline samples; after two weeks, samples of **1** undergo complete conversion to **2,** as indicated by the change in reflections located near 10° in 2θ in the powder XRD patterns (Figure 2). The full powder patterns

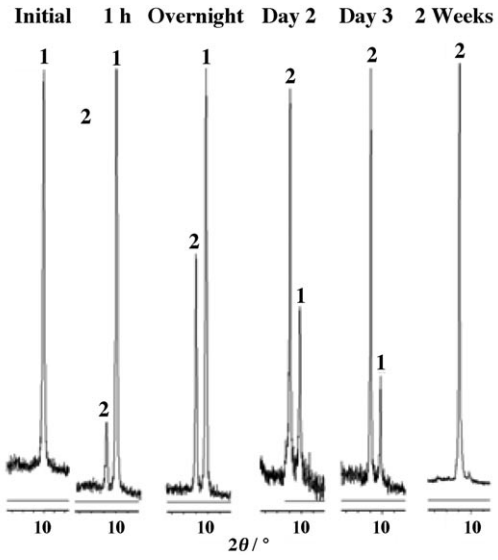

Figure 2. X-ray diffraction powder patterns in the 10° 2θ region of a sample of Tl(TCNQ) crystals after prolonged exposure to ambient laboratory air.

are provided in Figure S7 in the Supporting Information. It is important to emphasize that phase I (**1**) is indefinitely stable under dry conditions, and it is only upon exposure of the crystalline sample of **1** to a wet atmosphere that a transition in the solid state to phase II (**2**) is observed. The transformation of **1** to **2** is accelerated and takes only two hours when crystals of **1** are soaked in water (Figure S8 in the Supporting Information). The phase change occurs without any visible changes in the sample or soluble components. Given these observations, it is postulated that **1** is being essentially "dissolved" at the surface by atmospherically scavenged water, and that this process slowly converts the material to the second polymorph, that is, Phase II (**2**). The effects of other external stimuli, such as pressure and vacuum, were studied, but no changes in the structure were found to occur (Figure S9 in the Supporting Information). Experiments were performed to attempt to convert **2** back to **1** by exposing the solid to heat, pressure, and vacuum, but no alterations in the structure were observed, thus indicating that the transition is irreversible and that **2** is the thermodynamic product. Such a phase transformation at ambient temperatures and pressures and in the solid state without the loss or exchange of guest or interstitial solvent molecules is remarkable and, to our knowledge, unprecedented in metal–organic framework solids (MOFs).

Infrared spectroscopy is a useful tool for characterizing TCNQ materials, in particular for discerning the oxidation state of the molecule in its charge-transfer salts or metal–organic frameworks. Not unexpectedly, infrared spectra of the two polymorphs of Tl(TCNQ) are quite similar, given that they both contain the radical anion form of TCNQ. Compound **1** exhibits three strong, broad ν(C≡N) absorptions at 2181, 2164, and 2151 cm^{-1} whereas **2** exhibits a strong, sharp stretch at 2180 and one strong, broad feature at 2149 cm^{-1}. Perhaps even more indicative of the similarity of the TCNQ unit in the two phases is the δ(C–H) mode at 823 cm^{-1}, which is very sensitive to changes in oxidation state. These data are consistent with the presence of $TCNQ^-$ and not TCNQ, $TCNQ^{2-}$, or mixed-valence stacks of $TCNQ^-$ and TCNQ.[33–35]

Variable-temperature magnetic susceptibility data for the samples were measured using a SQUID magnetometer. Both polymorphs show behavior typical of a TCNQ radical anion salt with TCNQ stacking, namely strong coupling of the unpaired spins. Most simple TCNQ radical anion salts are paramagnetic, but the susceptibilities are only about 10% of that expected for a system with non-interacting spins.[21] The very low susceptibility observed for both polymorphs ($C =$ 0.009 for **1** and 0.0005 for **2**; Figure S11 in the Supporting Information) indicates considerable magnetic coupling of the unpaired spins through the TCNQ stacking interactions, as expected.

The two structural forms of Tl(TCNQ) were subjected to pressed-pellet conductivity measurements (Figure 3), and it was found that they exhibit quite different charge-transport properties. Both behave as semiconductors, but phase II (**2**) has a room-temperature conductivity of 5.4×10^{-1} S cm^{-1}, whereas phase I (**1**) is nearly insulating, with a room-temperature conductivity of only 2.4×10^{-4} S cm^{-1}. In contrast to the binary alkali-metal TCNQ materials, the Tl(TCNQ) polymorphs do not exhibit a phase transition as the temperature is decreased. Structurally, the polymorph **1** and Cu(TCNQ)

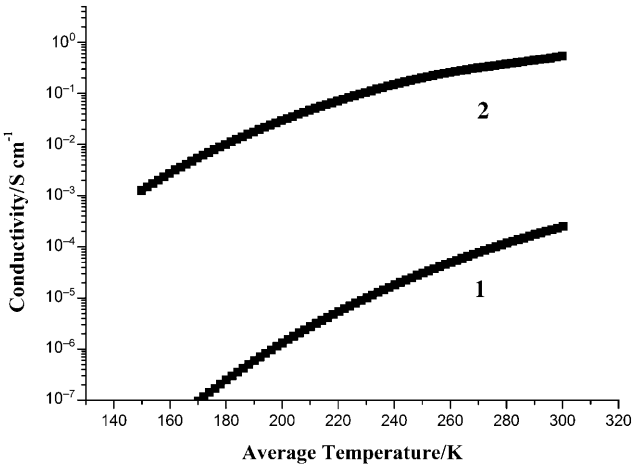

Figure 3. Conductivity measurements performed on pressed pellets of phase I (**1**) and phase II (**2**) of Tl(TCNQ).

phase I are very similar. As described earlier, both compounds contain metal ions which are connected to the TCNQ ligands in a μ_4 binding mode, with the stacks of TCNQ propagating along the short axis and the adjacent stacks rotated by 90°. Nevertheless, in comparison to Cu(TCNQ) phase I, **1** shows alternating distances between both TCNQ molecules along the stack (3.17(1) and 3.35(1) Å) and the adjacent Tl metal ions (3.63(1) and 3.45(1) Å). The alternating distances reflect a partial dimerization of the TCNQ radicals, which leads to the formation of a spin-Peierls insulator state and a relatively low conductivity. The structural features of **2** are in accord with the unusually high room-temperature conductivity of this material (5.4×10^{-1} S cm^{-1}). The distance between adjacent TCNQ radical ions is homogeneous (3.22(2) Å) and is slightly shorter than the TCNQ distance found in Cu(TCNQ) phase I (3.24 Å), which explains its superior semiconducting properties.

In summary, the results of this study establish the existence of two markedly different polymorphs of Tl-(TCNQ). Powder X-ray diffraction studies revealed that subtle differences in the reaction conditions (e.g. time and temperature; Figure S9 in the Supporting Information) lead to variable quantities of the two phases. With some effort, we were able to identify conditions that lead to pure samples of each polymorph (Figure S5 in the Supporting Information). Conductivity data obtained on pressed pellets of bulk samples of the two phases revealed that **1** is a weak semiconductor, a finding that is not unexpected given the pronounced π dimerization of the $TCNQ^-$ units along the stack. Conversely, polymorph **2** exhibits much higher conductivity as a result of the regular and short spacing between the $TCNQ^-$ units along the stack, in a situation that leads to increased electron mobility.

The results of this study add to the small database of single-crystal X-ray data available for binary TCNQ materials and provide valuable insight into structure–property relationships in such materials. Moreover, the Tl(TCNQ) solids constitute examples of new supramolecular main-group MOFs, an area of chemistry that has yet to be developed. Current efforts are underway to prepare additional members of this family with $TCNQX_2$ (X = Cl, Br, I) derivatives and to perform ^{205}Tl NMR and EPR spectroscopic measurements to probe the possible role of the Tl···Tl and TCNQ···TCNQ contacts as well as of the Tl–N bonding in dictating the properties. As a backdrop for these latter studies, we note that in their related work on the semiconductor $Tl(DM\text{-}DCNQI)_2$, Hünig et al. performed such NMR and EPR spectroscopy studies and were able to ascertain that, remarkably, spin density is transferred from the electron acceptors DM-DCNQI to the Tl metal ions.[25] Finally, this chemistry is being extended to other main-group elements to further expand knowledge in this new field of TCNQ conductors.

Experimental Section

1: A dark green solution of Li(TCNQ) (0.211 g, 1.0 mmol) in methanol (5 mL) was slowly added to a colorless solution of $TlPF_6$ (0.350 g, 1.0 mmol) in water (5 mL). The mixture was then diluted with water (10 mL) and stirred for 5 min. The resulting dark purple precipitate was quickly collected by filtration and subjected to immediate drying in vacuo. Yield = 0.113 g, 28 %. Single crystals of the compound were grown over the course of one week in a 3 mm diameter sealed thin tube by slow diffusion of a methanol solution of Li(TCNQ) into a solution of $TlPF_6$ in water. Elemental analysis calcd. for **1** $C_{14}N_4H_4Tl$: C 35.21, H 0.99, N 13.69; found: C 35.89, H 0.94, N 13.89 %. IR (Nujol): ν(C≡N) 2181, 2164, 2151, and δ(C–H) 823 cm^{-1}. Elemental and infrared spectral analyses were performed on single-crystal samples.

2: A dark blue solution of Li(TCNQ) (0.150 g, 0.7 mmol) in methanol (10 mL) was slowly added to a colorless solution of $TlPF_6$ (0.175 g, 0.5 mmol) in water (10 mL). The mixture was stirred in air for 20 min to yield a dark purple precipitate, which was filtered and washed with copious quantities of water and diethyl ether and dried in air. Yield = 0.180 g (0.41 mmol), 82 %. Elemental analysis calcd. for **2** $C_{14}N_4H_4Tl$: C 35.21, H 0.99, N 13.69; Found: C 35.83, H 0.98, N 13.90 %. IR(Nujol): ν(C≡N) 2180, 2149, and δ(C–H) 822 cm^{-1}.

Crystallographic parameters can be found in the Supporting Information (Table S1). CCDC 812759 (**1**) and 806915 (**2**) contain the supplementary crystallographic data for this paper. These data can be obtained free of charge from The Cambridge Crystallographic Data Centre via www.ccdc.cam.ac.uk/data_request/cif.

Received: January 15, 2011
Revised: March 8, 2011
Published online: June 7, 2011

Keywords: main group elements · metal–organic frameworks · polymorphism · semiconductors · thallium

[1] G. I. Meijer, *Science* **2008**, *319*, 1625.
[2] R. M. Metzger, *Chem. Rev.* **2003**, *103*, 3803.
[3] O. Sato, J. Tao, Y.-Z. Zhang, *Angew. Chem.* **2007**, *119*, 2200; *Angew. Chem. Int. Ed.* **2007**, *46*, 2152.
[4] O. Sato, T. Kawakami, M. Kimura, S. Hishiya, S. Kubo, Y. Einaga, *J. Am. Chem. Soc.* **2004**, *126*, 13176.
[5] H. Okamura, M. Matsubara, T. Nanba, T. Tayagaki, S. Mouri, K. Tanaka, Y. Ikemoto, T. Moriwaki, H. Kimura, G. Juhasz, *Phys. Rev. B* **2005**, *72*, 073108.
[6] H. Okamura, M. Matsubara, T. Tayagaki, K. Tanaka, Y. Ikemoto, H. Kimura, T. Moriwaki, T. Nanba, *J. Phys. Soc. Jpn.* **2004**, *73*, 1355.
[7] P. Batail, S. J. LaPlaca, J. J. Mayerle, J. B. Torrance, *J. Am. Chem. Soc.* **1981**, *103*, 951.
[8] J. B. Torrance, A. Girlando, J. J. Mayerle, J. L. Crowley, V. Y. Lee, P. Batail, S. J. LaPlaca, *Phys. Rev. Lett.* **1981**, *47*, 1747.
[9] R. M. Metzger, J. B. Torrance, *J. Am. Chem. Soc.* **1985**, *107*, 117.
[10] R. Kato, H. Kobayashi, A. Kobayashi, *J. Am. Chem. Soc.* **1989**, *111*, 5224.
[11] M. Nakano, M. Kato, K. Yamada, *Phys. Rev. B* **1993**, *186–188*, 1077.
[12] F. O. Karutz, J. U. von Schütz, H. Wachtel, H. C. Wolf, *Phys. Rev. Lett.* **1998**, *81*, 140.
[13] H. Schmitt, J. U. von Schütz, H. Wachtel, H. C. Wolf, *Synth. Met.* **1997**, *86*, 2257.
[14] J. U. von Schütz, D. Bauer, H. Wachtel, H. C. Wolf, *Synth. Met.* **1995**, *71*, 2089.
[15] J. U. von Schütz, D. Gomez, H. Wachtel, H. C. Wolf, *J. Chem. Phys.* **1996**, *105*, 6538.
[16] J. U. von Schutz, D. Gomez, H. Schmitt, H. Wachtel, *Synth. Met.* **1997**, *86*, 2095.
[17] A. Ota, H. Yamochi, G. Saito, *J. Mater. Chem.* **2002**, *12*, 2600.
[18] M. Chollet, L. Guerin, N. Uchida, S. Fukaya, H. Shimoda, T. Ishikawa, K. Matsuda, T. Hasegawa, A. Ota, H. Yamochi, G. Saito, R. Tazaki, S.-i. Adachi, S.-y. Koshihara, *Science* **2005**, *307*, 86.

[19] R. S. Potember, T. O. Poehler, D. O. Cowan, *Appl. Phys. Lett.* **1979**, *34*, 405.
[20] R. S. Potember, T. O. Poehler, R. C. Benson, *Appl. Phys. Lett.* **1982**, *41*, 548.
[21] R. A. Heintz, H. Zhao, X. Ouyang, G. Grandinetti, J. Cowen, K. R. Dunbar, *Inorg. Chem.* **1999**, *38*, 144.
[22] R. Kumai, Y. Okimoto, Y. Tokura, *Science* **1999**, *284*, 1645.
[23] M. A. McGuire, T. K. Reynolds, F. J. DiSalvo, *Chem. Mater.* **2005**, *17*, 2875.
[24] G. Bouhadir, D. Bourissou, *Chem. Soc. Rev.* **2004**, *33*, 210.
[25] S. Hünig, H. Meixner, T. Metzenthin, U. Langohr, J. U. von Schütz, H. C. Wolf, E. Tillmanns, *Adv. Mater.* **1990**, *2*, 361.
[26] M. A. Pitt, D. W. Johnson, *Chem. Soc. Rev.* **2007**, *36*, 1441.
[27] M. K. Kim, Y. I. Kim, S. B. Moon, S. N. Choi, *Bull. Korean Chem. Soc.* **1996**, *17*, 424.
[28] M. C. Grossel, S. C. Weston, *J. Chem. Soc. Chem. Commun.* **1992**, 1510.
[29] J. Janczak, R. Kubiak, *J. Alloys Compd.* **1993**, *202*, 69.
[30] L. Shields, *J. Chem. Soc. Faraday Trans. 2* **1985**, *81*, 1.
[31] M. Konno, Y. Saito, *Acta Crystallogr. Sect. B* **1974**, *30*, 1294.
[32] H. Kobayashi, *Bull. Chem. Soc. Jpn.* **1981**, *54*, 3669.
[33] M. Inoue, M. B. Inoue, *J. Chem. Soc. Faraday Trans. 2* **1985**, *81*, 539.
[34] M. Inoue, M. B. Inoue, *Inorg. Chem.* **1986**, *25*, 37.
[35] M. B. Inoue, M. Inoue, Q. Fernando, K. W. Nebesny, *J. Phys. Chem.* **1987**, *91*, 527.

